# Supporting Information

# Multistage extraction platform for highly efficient and fully continuous purification of nanoparticles

Yi Shen [a,‡], Nopphon Weeranoppanant [a,b,‡], Lisi Xie [a], Yue Chen [c], Marcella R. Lusardi [d], Joseph Imbrogno [a], Moungi G. Bawendi [c,*] and Klavs F. Jensen [a,d,*]

[a] Department of Chemical Engineering, [c] Department of Chemistry, [d] Department of Materials Science and Engineering, Massachusetts Institute of Technology, Cambridge, MA 02139, United States
[b] Present address: Department of Chemical Engineering, Burapha University, Chonburi, Thailand, 20130
*Corresponding authors: mgb@mit.edu; kfjensen@mit.edu.
‡ YS and NW contributed equally.

## Detailed Description of membrane separator module

The multistage extraction platform was a cascade of extraction modules, each of which consisted of mass transfer tubing and a separator. The length of the mass transfer tubing was selected based on the mass transfer coefficient ($k_La$) for segmented flow, which was reported to be 0.2-1.0 s$^{-1}$. Therefore, a characteristic time for mass transfer was approximately 1-5 seconds. The flow rate we chose to use in this work is 1 mL/min, and the length of the tubing (0.03" ID, 1/16" OD) we used was 35 cm long. The residence time inside the mass transfer tubing is 10 s (20 s for the scale up test on the concentrated CdSe QD solution experiment), which is twice the upper bound of the time required for a typical mass transfer process for segmented flow. We did not observe any increase in the percentage extraction on the one-stage methanol extracting CdSe QD solution experiment with an increase residence time (1 min).
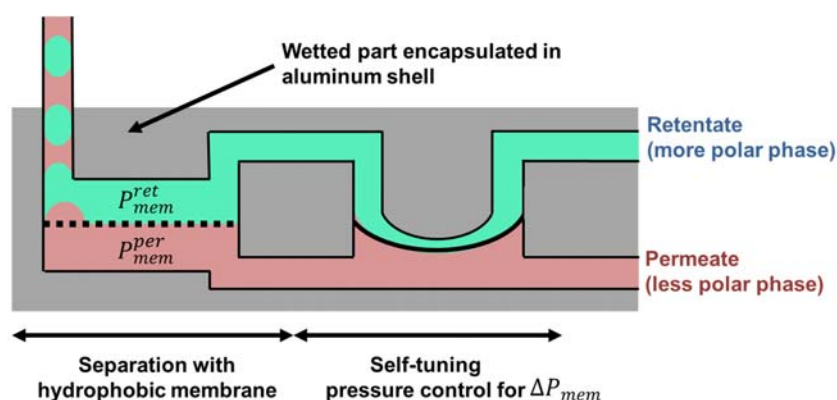


**Figure S1.** Drawing of the extraction module

As shown in Figure S1, the membrane separator was similar to the previous design[1]. However, the separator was now machined in ultra-high-molecular-weight polyethylene for the inner part, which would be wetted and in contact with organic solvents. The part was encapsulated in an outer shell made of aluminum. The separator had two important elements: (a) microporous polymer membrane

and (b) self-tuning pressure control. We selected the membrane materials based on their reported

chemical compatibility with solvents (e.g. octane, methanol, DMF). The membrane we chose to use is

a 0.5 μm-pore PTFE membrane with a PTFE support layer (PTFE/PTFE, membrane thickness 178

μm). The membrane has hydrophobic PTFE as an active layer, which allows a less polar phase to

permeate through and provides excellent compatibility with all the chemicals in the system.
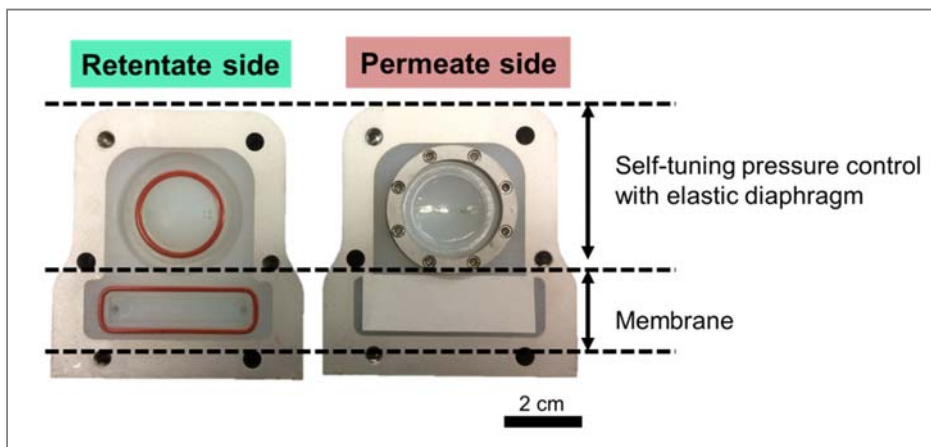


**Figure S2**. Image of the membrane separator with wetted and shell parts made of polyethylene and
aluminum, respectively.

To achieve complete phase separation in the separator, we need to ensure pressure balance

across the membrane ($\Delta P_{mem} = P_{mem}^{ret} - P_{mem}^{per}$). If $\Delta P_{mem}$ is too high, then the more polar phase can

breakthrough into the permeate side. On the other hand, if $\Delta P_{mem}$ is too low, then the less polar phase

can partially be retained with the retentate side. For successful operation, $\Delta P_{mem}$ has to be

maintained within lower and upper limits[2,3]. The lower limit ($\Delta P_{per}$) corresponds to a minimum pressure

drop to force all the less polar phase to permeate through the membrane, which is estimated by

assuming a cylindrical shape of the membrane pore and using a Hagen-Poiseuille equation. The upper

limit ($\Delta P_{cap}$) is associated with capillary pressure. As shown in Table S1, in order to obtain these two values, physical properties of the liquid-liquid systems such as interfacial tensions and contact angles are needed.

**Table S1**. The two pressure limits on $\Delta P_{mem}$ to ensure complete phase separation. $\Delta P_{per}$ and $\Delta P_{cap}$ represent the lower and upper limits, respectively.

| $\Delta P_{per}$ | $\Delta P_{cap}$ |
|:---:|:---:|
| $$\Delta P_{per} = \frac{8\mu_{per}\left(\frac{Q_{per}}{n_{pore}}\right)L_{pore}}{\pi R_{pore}^4}$$ | $$\Delta P_{cap} = \frac{2\gamma\cos(\theta)}{R_{pore}}$$ |
| $\mu_{per}$= Viscosity of the permeate phase (mPa.s) | $\gamma$= Interfacial tension between the two liquid phase (mN/m) |
| $Q_{per}$= Volumetric flow rate of the permeate phase (mL/min) | $\theta$= Contact angle between the two liquid phases and membrane |
| $n_{pore}$= Pore number density of the membrane | $R_{pore}$= Radius of the membrane pore (μm) |
| $L_{pore}$= Thickness of the membrane (μm) | |
| $R_{pore}$= Radius of the membrane pore (μm) | |

# Interfacial tension and contact angle measurements

The interfacial tensions were measured using a drop shape analyzer (DSA100, Krüss) with a pendant drop method. The contact angles were measured by depositing a drop of the heavy phase in the light phase and onto the PTFE membrane surface. Note that we did not study the interfacial properties of the octane-acetonitrile system because the preliminary NMR showed poor percent extraction with acetonitrile. As another required liquid property, the viscosity of the permeate phase ($\mu_{per}$) was assumed to be that of pure octane. These numbers were listed in **Table S2**.

**Table S2.** Properties of the two liquid-liquid systems used in the CdSe purification

|  |  | Octane – methanol [a] | Octane – DMF [a] |
| --- | --- | --- | --- |
| $\mu_{per}$ | Nominal | 0.51 mPa.s | 0.51 mPa.s |
| $\rho_{permeate}$ | Measured | 0.7041 g/mL | 0.7095 g/mL |
| $\rho_{retentate}$ | Measured | 0.7656 g/mL | 0.9148 g/mL |
| $\gamma$ | Measured | 0.97 mN/m | 2.36 mN/m |
| $\theta$ | Measured | 34.7° | 43.1° |

[a] "Octane-methanol" and "Octane-DMF" refer to the systems containing the feed solution (CdSe in octane) and extraction solvent (methanol or DMF) in a 1:1 v/v ratio.

With those values, we calculated the lower limit $\Delta P_{per}$ and upper limit $\Delta P_{cap}$ for two liquid-liquid extraction systems. Note that $\Delta P_{per}$ is dependent on flow rate. In this calculation, we assume flow

rate of the permeate phase is 0.5 mL/min. Therefore, the pressure balance operating window for the

membrane separation is 0.021 psi to 0.93 psi for the octane-methanol system and 0.021 psi to 2.00

psi for the octane-DMF system. Therefore, we designed the self-tuning pressure control such that it

provided a fixed pressure $(P_{dia})$ for $\Delta P_{mem}$ to be about 0.4-0.6 psi. With this design specification, we

observed successful phase separation with this design throughout all experiments.

# Preparation and characterization of CdSe and Au nanoparticles

**Materials and analytical methods**

Cadmium oxide (99.99%), oleic acid (90%), selenium powder (>99.5%) sodium borohydride and ferrocene (98%) were purchased from Sigma Aldrich. Hydrogen tetrachloroaurate (III) hydrate (99.8%-Au), trioctylphosphine (97%) were purchased from Strem Chemicals. mPEG-SH (MW 2000) was purchased from Laysan Bio. Toluene-$d_8$ (D, 99.5%) was obtained from Cambridge Isotope Laboratories. Bio-Beads S-X1 GPC medium was purchased from Bio-Rad Laboratories. All the chemicals were used as received.

UV-Vis spectra were taken in Shimadzu UV-3101PC UV-VIS-NIR scanning spectrometer. Transmission electron microscopy (TEM) images were recorded with a JEOL 2010 Advanced High Performance microscope. The quantitative $^1$H NMR spectra were recorded on Bruker Avance-400 NMR spectrometer with ferrocene as the internal standard and 30 s relaxation delay. The concentration of CdSe QDs for typical measurement is above 100 µM to increase the signal-to-noise-ratio. $^{31}$P NMR spectra were recorded on Varian Inova-500 NMR spectrometer.

**Synthesis of the oleate capped CdSe QDs.**

The oleate capped CdSe QDs were prepared in the high temperature (HT) / high pressure (HP) tube reactor as reported previously[4]. The HT/HP reactor was made by super-smooth stainless steel tubes purchased from McMaster-Carr (type 304 stainless steel, OD=1/16'', ID=0.02''). The reactor volume

was approximately 355 uL. The tubes were wrapped around an aluminum rod (OD=2'') with a heating cartridge inserted into the center of the rod. All connections, tubes, and devices were made out of type-316 stainless steel, and heating cartridges were made of multipurpose aluminum. The precursor solutions were injected by two syringe pumps (Harvard apparatus, PhD Ultra).

Cd(Oleate)$_2$ was used as the Cd precursor, which was synthesized and purified following a reported method[5]. The Cd precursor stock solution was prepared by dissolving 3.37g Cd(Oleate) in 48mL octane with 2mL TOP to improve mixing. The selenium precursor stock solution was prepared by diluting 2.27mL TOPSe (2.2M) solution into 47.7mL octane. The concentration of both precursor solution was 100mM. All precursor-handling processes were carried out inside the glovebox.

The synthesis of QDs was performed at 850 psi at 270 °C under nitrogen. The flow rate of each precursor was 50μL/min. Considering the effect of the solvent expansion, the residence time inside the tube reactor is around 2.4 min. The first absorption peak is at 544nm. The as-synthesized solution was diluted to around 13 μM based on the absorption spectra before use in LLE purification.

**Synthesis of the thiol-PEG capped Au nanoparticles**

10 mg of chloroauric acid was dissolved in 10 mL DI water, and 200 μL 0.2 M sodium hydroxide aqueous solution was then added under stirring. 24 mg mPEG-SH (MW 2000) was dissolved in 1 mL DI water and added to the above solution. After 5 min of stirring, 2 mg sodium borohydride in 0.7 mL DI water solution was added drop-wise, and the reaction was kept stirring at room temperature for 3 hours.

**Purification of CdSe QDs by gel permeation chromatography (GPC)**

The preparative GPC column was packed following a previously reported procedure[6]. 4g of swollen bio-beads were transferred to a glass column with a filter and glass frit disk. After the gel settled down and formed a column with approximately 28 mL volume, a small layer of sand was carefully placed at the top of the column rinsed by toluene. The as-synthesized CdSe QDs were pumped dry and redispersed in toluene. The CdSe QD toluene solution was then injected into the column, and all the purified samples were collected when the elution volume was close to 1/3 of the total volume of the column. The collected samples were used for the NMR ligand population study.

**Thermogravimetric analysis (TGA) of the nanoparticles**

The nanoparticle solutions were first concentrated and dropcasted onto a platinum pan in liquid form for the TGA characterization. The measurement was conducted on Discovery Thermogravimetric Analyzer (TA instruments) with isothermal at 50 °C and a heating rate of 5~10 °C/min to 600~700 °C under $N_2$ flow.

**Headspace gas chromatography (HS-GC) measurement**

The remaining residual amount of methanol after LLE was determined by Headspace gas chromatograph so that CdSe QD samples were not directly injected into the column. The sample solution was prepared by adding 50 µL into 5 mL of dimethylacetamide (DMA). The samples were transferred to a 20-mL headspace vial with a crimp cap. The HSGC system used was an Agilent model

7890 gas chromatograph equipped with a flame ionization detection (FID) system and a G1888 autosampler controlled by ChemStation software. In the headspace unit, the samples were allowed to equilibrate for 8 min at 100 °C. The column was J&W 122-1334 (30m x 250 μm x 1.4 μm). For the oven, the temperature profile started at 70 °C and held for 1 min. Then, the oven temperature was ramped up at the rate of 10°C/min until it reached 220 °C. The total GC cycle time was 22.5 min.

**Photoluminescence quantum yield**

According to the literature, purification of quantum dots can affect the brightness of the samples[7]. In this work, the quantum yields (QYs) of CdSe QDs purified by different methods were measured. Quantum yield measurements were carried out using a 405 nm diode laser and an integrating sphere (Labsphere RTC-060-SF). The excitation beam was blocked by a colored glass longpass filter (490 nm. The QY of the as-synthesized CdSe QD sample was 7%. The QY decreased to 4% after extracting batch wise twice with methanol (S/F = 1). When we used the same amount of methanol to perform 2 times PR on the sample (with the addition of acetone), the QY dropped to 2%. Since the brightness of the CdSe QDs is sensitive to the ligand population on the surface, this result suggests that LLE is a milder purification method compared to the PR technique.
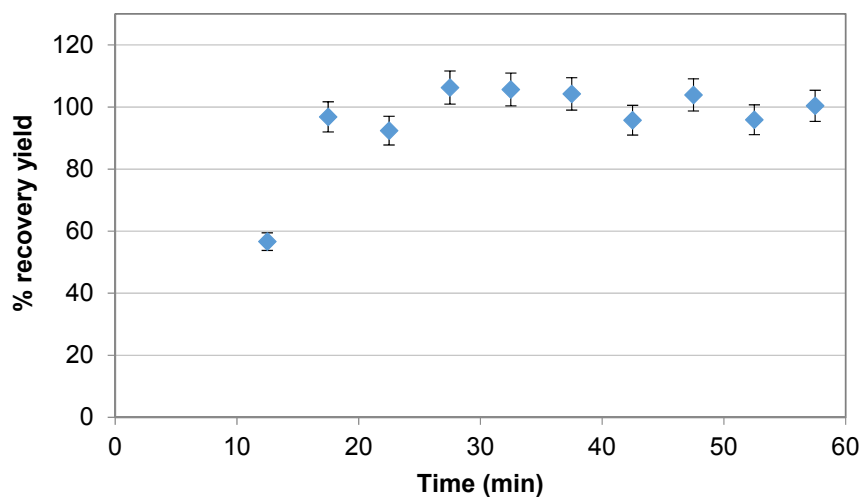
**Figure S3**
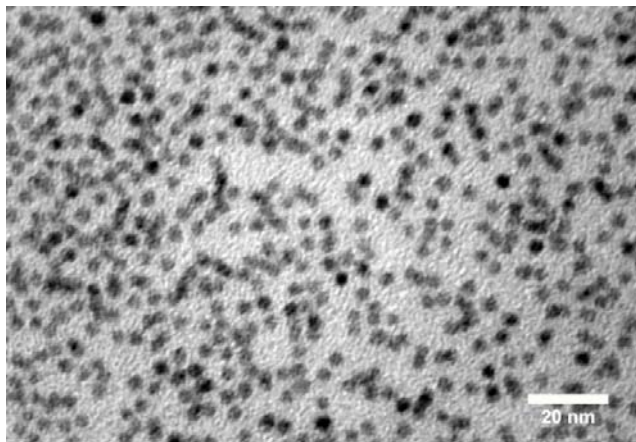


TEM image of the LLE purified CdSe QDs (prepared by Exp. F).

# Figure S4

To determine the steady state, the recovered phase outlet was sampled at different time points. Each sample was then measured with UV absorption to obtain the concentration of CdSe QDs. The recovery yield is the amount of CdSe nanoparticles being recovered in the recovered phase relative to the original amount at the inlet flow, and mathematically defined as follows:

$$Recovery\ yield = \frac{[CdSe]_{Recovery} * Q_{Recovery}}{[CdSe]_{Feed} * Q_{Feed}}$$

Here Q is the flow rate. We assume systematic error bars of 5% on the calculated recovery yield. The deviation may be from the syringe pump as well as UV absorption measurement. The results from the multistage extraction platform show close 100% recovery yield over continuous operations, regardless of the number of stages. For example, Figure S4 shows the percent recovery yields over time for Exp.F, maintaining around 100%. The results of other experiments are summarized below (Note that the uncertainties are estimated from the standard deviations of the percent recovery yields at multiple time points after steady state from the same experiment).
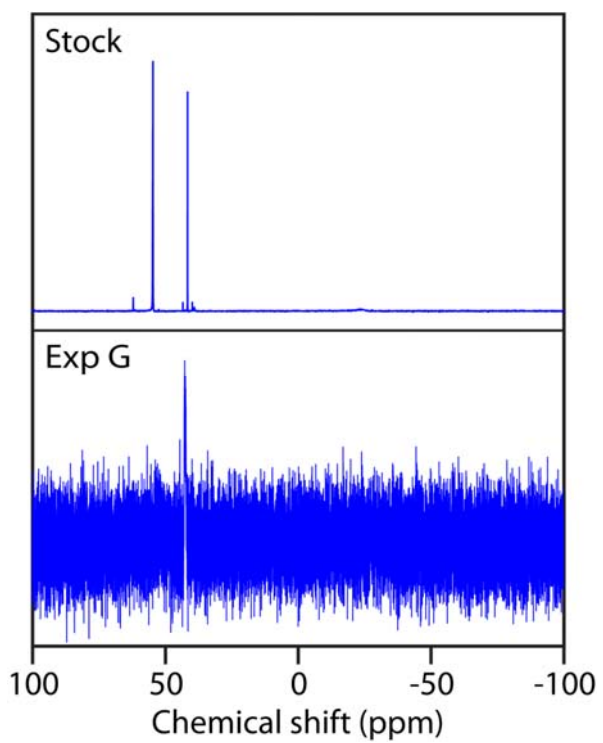


**Figure S4** Profile of percentage recovery yield of CdSe QDs over different time points for Exp. F

**Table S3.** Percentage recovery yield under different experimental conditions

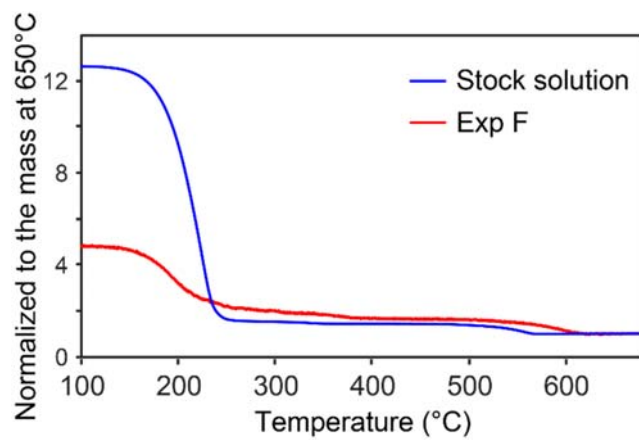| Exp. | Overall recovery yield |
|:---:|:---:|
| A | (96 ± 7)% |
| B | (102 ± 2)% |
| C | (99 ± 5)% |
| D | (96 ± 4)% |
| E | (98 ± 4)% |
| F | (100 ± 5)% |

**Figure S5**



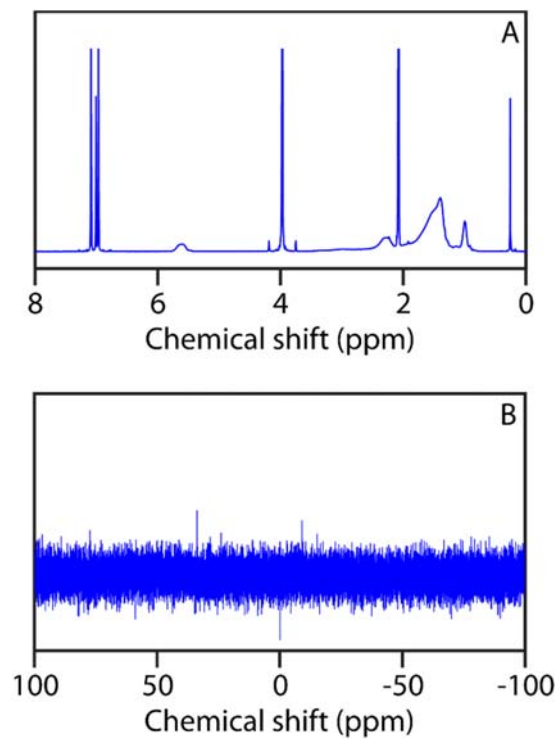$^{31}$P NMR spectra of the CdSe stock solution and the LLE purified solution through experiment G. Similar to the $^1$H NMR result, the removal of the peaks in the spectra suggests that the CdSe QD solution has been purified.
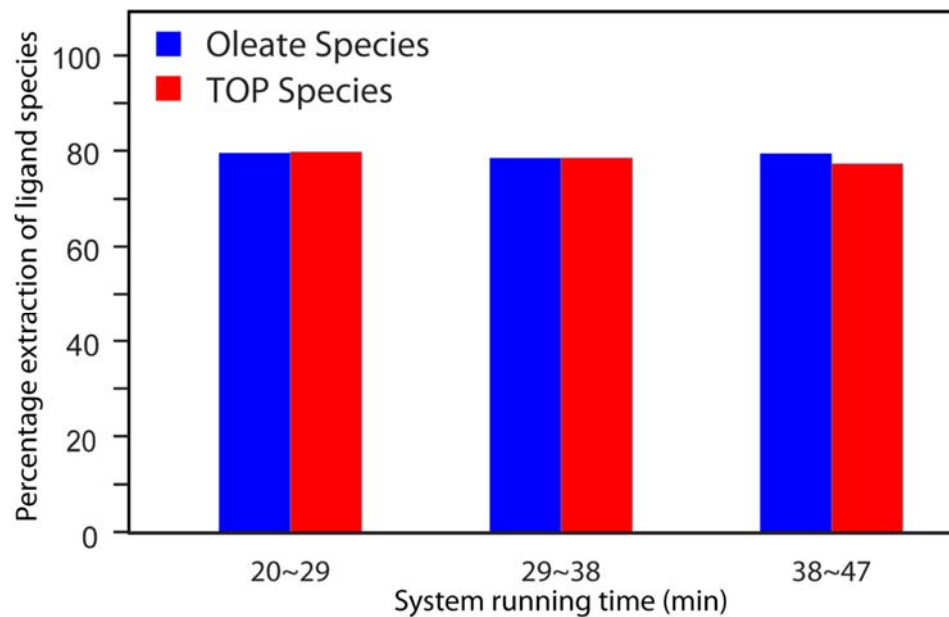
**Figure S6**



TGA curves of the stock (blue) and LLE purified (red, Exp. F) CdSe QD samples.
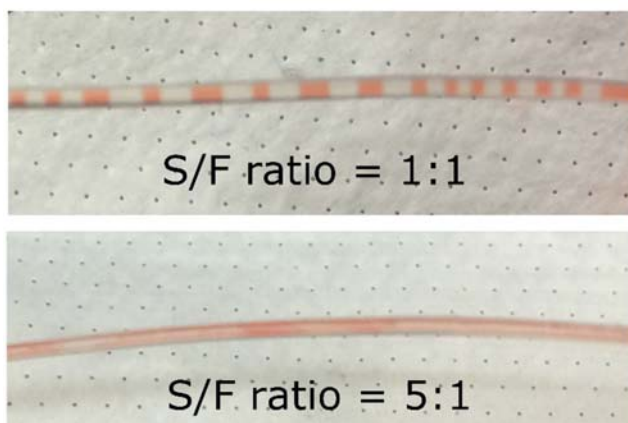
**Figure S7**



$^1$H NMR (A) and $^{31}$P NMR (B) spectra of the GPC purified CdSe QD solution. The impurities were considered to be fully removed in this sample.
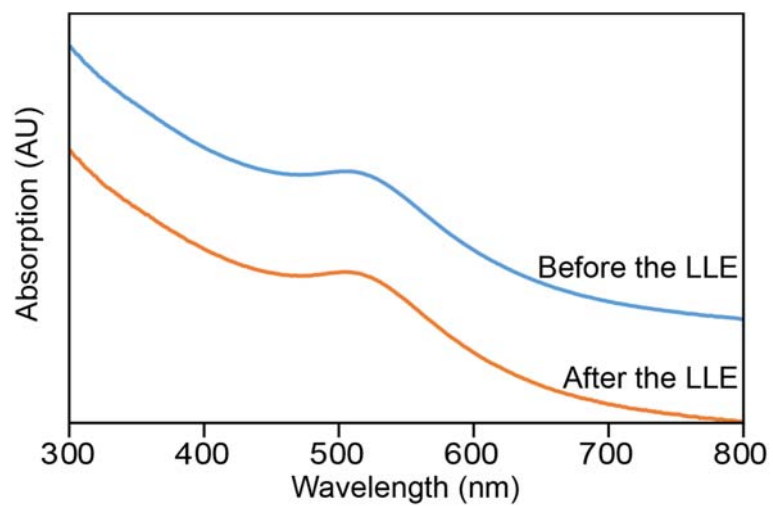
**Figure S8**



Ligand removal study of the LLE purified CdSe QDs with respect to the system running time under the following condition: methanol extracting, S/F = 1, N = 5. The constant percentage extraction of ligand species during this time period suggests the high durability and reproducibility of the LLE set up.
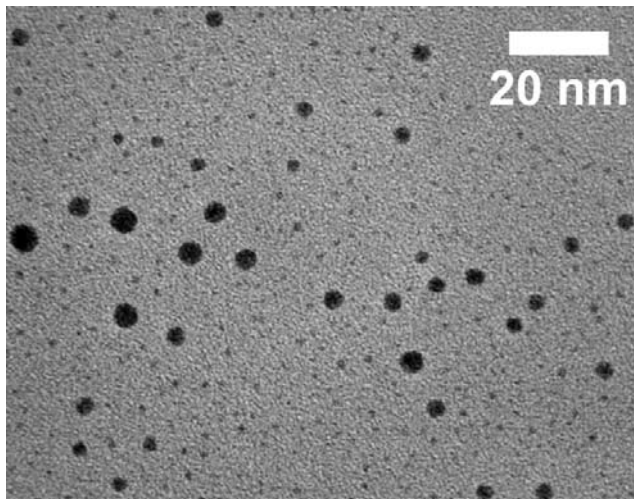
**Figure S9**



Pictures of the flow pattern at different S/F ratios. When the S/F ratio is low (1:1), segmented flow was observed. However, if the S/F ratio is too high (5:1), octane and methanol become miscible and the CdSe QD precipitated inside the tubing.

**Figure S10**



Absorption spectra of Au nanoparticles before (blue) and after (red) LLE purification.

**Figure S11**



TEM image of the LLE purified Au nanoparticle sample.

# References

1   A. Adamo, P. L. Heider, N. Weeranoppanant and K. F. Jensen, Ind. Eng. Chem. Res., 2013, 52, 10802–10808.

2   A. Günther, M. Jhunjhunwala, M. Thalmann, M. A. Schmidt and K. F. Jensen, Langmuir, 2005, 21, 1547–1555.

3   J. G. Kralj, H. R. Sahoo and K. F. Jensen, Lab Chip, 2007, 7, 256–263.

4   L. Xie, Y. Shen, D. Franke, V. Sebastián, M. G. Bawendi and K. F. Jensen, J. Am. Chem. Soc., 2016, 138, 13469–13472.

5   R. García-Rodríguez and H. Liu, Chem. Commun., 2013, 49, 7857–7859.

6   Y. Shen, M. Y. Gee, R. Tan, P. J. Pellechia and A. B. Greytak, Chem. Mater., 2013, 25, 2838–2848.

7   Y. Shen, M. Y. Gee and A. B. Greytak, Chem. Commun., 2017, 53, 827–841.